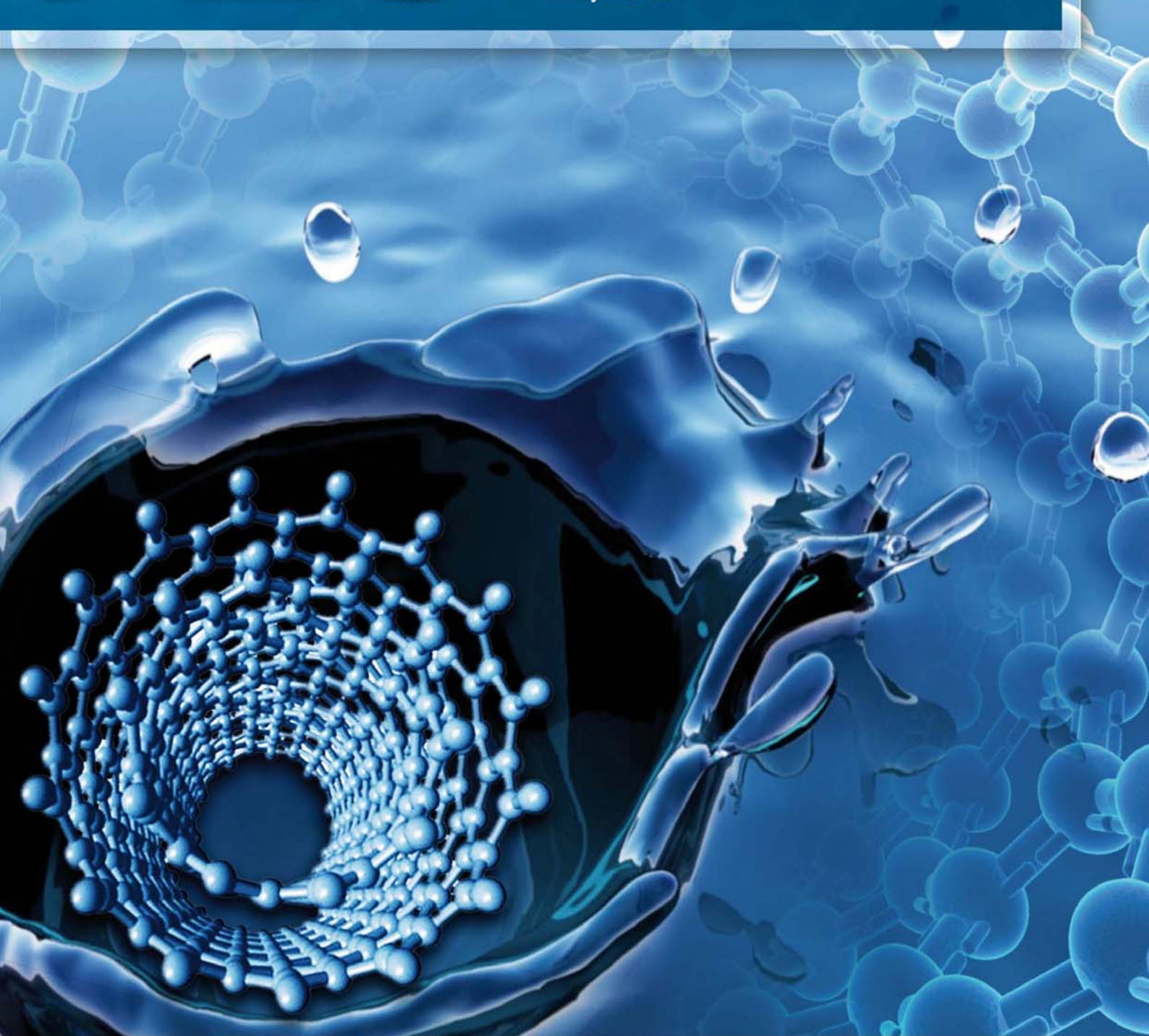


JES

JOURNAL OF
ENVIRONMENTAL
SCIENCES

ISSN 1001-0742
CN 11-2629/X

July 1, 2013 Volume 25 Number 7
www.jesc.ac.cn



Sponsored by
Research Center for Eco-Environmental Sciences
Chinese Academy of Sciences

CONTENTS

Aquatic environment

- Application potential of carbon nanotubes in water treatment: A review
Xitong Liu, Mengshu Wang, Shujuan Zhang, Bingcai Pan 1263
- Characterization, treatment and releases of PBDEs and PAHs in a typical municipal sewage treatment plant situated beside an urban river, East China
Xiaowei Wang, Beidou Xi, Shouliang Huo, Wenjun Sun, Hongwei Pan, Jingtian Zhang, Yuqing Ren, Hongliang Liu 1281
- Factors influencing antibiotics adsorption onto engineered adsorbents
Mingfang Xia, Aimin Li, Zhaolian Zhu, Qin Zhou, Weiben Yang 1291
- Assessment of heavy metal enrichment and its human impact in lacustrine sediments from four lakes in the mid-low reaches of the Yangtze River, China
Haijian Bing, Yanhong Wu, Enfeng Liu, Xiangdong Yang 1300
- Biodegradation of 2-methylquinoline by *Enterobacter aerogenes* TJ-D isolated from activated sludge
Lin Wang, Yongmei Li, Jingyuan Duan 1310
- Inactivation, reactivation and regrowth of indigenous bacteria in reclaimed water after chlorine disinfection of a municipal wastewater treatment plant
Dan Li, Siyu Zeng, April Z. Gu, Miao He, Hanchang Shi 1319
- Photochemical degradation of nonylphenol in aqueous solution: The impact of pH and hydroxyl radical promoters
Aleksandr Dulov, Niina Dulova, Marina Trapido 1326
- A pilot-scale study of cryolite precipitation from high fluoride-containing wastewater in a reaction-separation integrated reactor
Ke Jiang, Kanggen Zhou, Youcai Yang, Hu Du 1331

Atmospheric environment

- Effect of phosphogypsum and dicyandiamide as additives on NH₃, N₂O and CH₄ emissions during composting
Yiming Luo, Guoxue Li, Wenhai Luo, Frank Schuchardt, Tao Jiang, Degang Xu 1338
- Evaluation of heavy metal contamination hazards in nuisance dust particles, in Kurdistan Province, western Iran
Reza Bashiri Khuzestani, Bubak Sourì 1346

Terrestrial environment

- Utilizing surfactants to control the sorption, desorption, and biodegradation of phenanthrene in soil-water system
Haiwei Jin, Wenjun Zhou, Lizhong Zhu 1355
- Detoxifying PCDD/Fs and heavy metals in fly ash from medical waste incinerators with a DC double arc plasma torch
Xinchao Pan, Jianhua Yan, Zhengmiao Xie 1362
- Role of sorbent surface functionalities and microporosity in 2,2',4,4'-tetrabromodiphenyl ether sorption onto biochars
Jia Xin, Ruilong Liu, Hubo Fan, Meilan Wang, Miao Li, Xiang Liu 1368

Environmental biology

- Systematic analysis of microfauna indicator values for treatment performance in a full-scale municipal wastewater treatment plant
Bo Hu, Rong Qi, Min Yang 1379
- Function of *arsATorf7orf8* of *Bacillus* sp. CDB3 in arsenic resistance
Wei Zheng, James Scifleet, Xuefei Yu, Tingbo Jiang, Ren Zhang 1386
- Enrichment, isolation and identification of sulfur-oxidizing bacteria from sulfide removing bioreactor
Jianfei Luo, Guoliang Tian, Weitie Lin 1393

Environmental health and toxicology

- In vitro* immunotoxicity of untreated and treated urban wastewaters using various treatment processes to rainbow trout leucocytes
François Gagné, Marlène Fortier, Michel Fournier, Shirley-Anne Smyth 1400
- Using lysosomal membrane stability of haemocytes in *Ruditapes philippinarum* as a biomarker of cellular stress
to assess contamination by caffeine, ibuprofen, carbamazepine and novobiocin
Gabriela V. Aguirre-Martínez, Sara Buratti, Elena Fabbri, Angel T. DelValls, M. Laura Martín-Díaz 1408

Environmental catalysis and materials

- Effect of transition metal doping under reducing calcination atmosphere on photocatalytic
property of TiO₂ immobilized on SiO₂ beads
Rumi Chand, Eiko Obuchi, Katsumi Katoh, Hom Nath Luitel, Katsuyuki Nakano 1419
- A high activity of Ti/SnO₂-Sb electrode in the electrochemical degradation of 2,4-dichlorophenol in aqueous solution
Junfeng Niu, Dusmant Maharana, Jiale Xu, Zhen Chai, Yueping Bao 1424
- Effects of rhamnolipid biosurfactant JBR425 and synthetic surfactant Surfynol465 on the
peroxidase-catalyzed oxidation of 2-naphthol
Ivanec-Goranina Rūta, Kulys Juozas 1431

The 8th International Conference on Sustainable Water Environment

- An novel identification method of the environmental risk sources for surface water pollution accidents in chemical industrial parks
Jianfeng Peng, Yonghui Song, Peng Yuan, Shuhu Xiao, Lu Han 1441
- Distribution and contamination status of chromium in surface sediments of northern Kaohsiung Harbor, Taiwan
Cheng-Di Dong, Chiu-Wen Chen, Chih-Feng Chen 1450
- Historical trends in the anthropogenic heavy metal levels in the tidal flat sediments of Lianyungang, China
Rui Zhang, Fan Zhang, Yingjun Ding, Jinrong Gao, Jing Chen, Li Zhou 1458
- Heterogeneous Fenton degradation of azo dyes catalyzed by modified polyacrylonitrile fiber Fe complexes:
QSPR (quantitative structure property relationship) study
Bing Li, Yongchun Dong, Zhizhong Ding 1469
- Rehabilitation and improvement of Guilin urban water environment: Function-oriented management
Yuansheng Pei, Hua Zuo, Zhaokun Luan, Sijia Gao 1477
- Adsorption of Mn²⁺ from aqueous solution using Fe and Mn oxide-coated sand
Chi-Chuan Kan, Mannie C Aganon, Cybelle Morales Futalan, Maria Lourdes P Dalida 1483
- Degradation kinetics and mechanism of trace nitrobenzene by granular activated carbon enhanced
microwave/hydrogen peroxide system
Dina Tan, Honghu Zeng, Jie Liu, Xiaozhang Yu, Yanpeng Liang, Lanjing Lu 1492

Serial parameter: CN 11-2629/X*1989*m*237*en*P*28*2013-7



Adsorption of Mn^{2+} from aqueous solution using Fe and Mn oxide-coated sand

Chi-Chuan Kan^{1,*}, Mannie C Aganon¹, Cybelle Morales Futalan², Maria Lourdes P Dalida³

1. Institute of Hot Spring Industry, Chia Nan University of Pharmacy and Science, Taiwan, China
2. Environmental Engineering Unit, University of Philippines Diliman, Quezon City, Philippines
3. Department of Chemical Engineering, University of Philippines Diliman, Quezon City, Philippines

Abstract

The adsorption of Mn^{2+} onto immobilized Mn-oxide and Fe-oxide adsorbent such as manganese oxide-coated sand1 (MOCS1), manganese oxide-coated sand2 (MOCS2), iron oxide-coated sand2 (IOCS2), and manganese and iron oxide-coated sand (MIOCS) was investigated. The effects of pH (5.5 to 8.0) and temperature (25 to 45°C) on the equilibrium capacity were examined. Equilibrium studies showed that there is a good fit with both Freundlich and Langmuir isotherm, which indicates surface heterogeneity and monolayer adsorption of the adsorbents. Kinetic data showed high correlation with the pseudo second-order model, which signifies a chemisorption-controlled mechanism. The activation energies, activation parameters (ΔG^* , ΔH^* , ΔS^*), and thermodynamic parameters (ΔG^0 , ΔH^0 , ΔS^0) confirmed that adsorption with MIOCS was endothermic and more spontaneous at higher temperature while an opposite trend was observed for the other adsorbents. Thermodynamic studies showed that adsorption involved formation of activated complex, where MOCS1 and MIOCS follow a physical-chemical mechanism, while MOCS2 and IOCS2 follows purely chemical mechanism.

Key words: activation energy; iron oxide; kinetics; manganese oxide; thermodynamics

DOI: 10.1016/S1001-0742(12)60188-0

Introduction

Manganese, one of the most abundant minerals in the earth's crust, is naturally present in groundwater and surface water. In groundwater, manganese occurs as a divalent ion (Mn^{2+}) in the form of hydroxides, sulfates, or carbonates under anoxic conditions. A Mn^{2+} concentration greater than 0.1 mg/L could lead to water discoloration, undesirable taste, and unpleasant odor in the water making it unsuitable for drinking. Upon exposure to air, Mn^{2+} forms MnO_2 particulates that can cause black or brown stains on household utensils, plumbing fixtures and clothing (Teng et al., 2001). For drinking water, the recommended maximum contaminant level of Mn^{2+} by US Environmental Protection Agency is 0.1 mg/L (Ellis et al., 2000).

Current technologies utilized for Mn removal include filtration, membrane processes, adsorption, ion exchange, precipitation, and chemical feed systems. Adsorption is an effective purification and separation process used in wastewater treatment particularly in heavy metal removal. Compared to precipitation-based technologies, adsorption can remove heavy metals over a wider pH range and at lower concentrations (Han et al., 2006; Benjamin et al., 1996).

Iron and manganese oxides are well-known to be effective adsorbents in heavy metal removal due to its microporous structure and high surface area. In addition, oxides of iron and manganese also possess hydroxide ($-OH$) functional groups (Han et al., 2006). The presence of MnO_2 on the oxide surface has a catalytic effect in the removal of Mn^{2+} (Phatai et al., 2010).

However, the application of oxides as an adsorbent or filter media is limited due to their physical properties such as bulky, amorphous, hydrated, and with low hydraulic conductivities (Benjamin et al., 1996). Iron and manganese oxides exist in different forms such as fine powder, suspended flocs or hydrogel, which makes solid/liquid separation more difficult (Han et al., 2006). In order to improve the mechanical stability, metal oxides are coated onto a more stable, granular media such as bentonite, zeolite, sericite, and silica sand. Previous studies showed the ability of Fe and/or Mn oxide-coated media in the adsorptive removal of As(III), As(V), Cu, Pb and Cr (Chang et al., 2008; Lai et al., 2000; Lee et al., 2004; Han et al., 2006; Tiwari et al., 2011; Li et al., 2009). Benjamin et al. (1996) reported the capability of iron oxide-coated sand in adsorbing uncomplexed and ammonia-complexed Cu, Cd, Pb, Ni, and Zn, as well as oxyanionic metals such as AsO_3 and SeO_3 , which shows the ability of Fe oxides in

* Corresponding author. E-mail: cckanev@mail.chna.edu.tw

removing anionic and cationic contaminants.

However, studies were limited in the removal of Mn^{2+} at high concentration using Mn oxide-coated media (Hu et al., 2004; Kim et al., 2009; Piispanen and Sallanko, 2010; Taffarel and Rubio, 2010) and Fe oxide-coated media (Buamah et al., 2008). Therefore, in order to understand the behavior of Fe and Mn oxide in the adsorptive removal of dilute Mn^{2+} from aqueous solution, further studies are necessary.

In this present study, the removal of Mn^{2+} using iron oxide and manganese oxide-coated sand was investigated. Five adsorbents were utilized and these were generally referred to as “greensand”. Each adsorbent contained a different composition of oxide in the coating depending on the manner in which they were synthesized: four adsorbents namely manganese oxide-coated sand1 (MOCS1), manganese oxide-coated sand2 (MOCS2), iron oxide-coated sand1 (IOCS1), and iron oxide coated sand2 (IOCS2) were synthesized using different oxide impregnation methods. On the other hand, manganese and iron oxide-coated sand (MIOCS), was obtained from the groundwater treatment plant. The study aims to examine the effect of pH and temperature on the removal of Mn^{2+} using iron oxide and manganese oxide-coated sand. The equilibrium data were analyzed using Langmuir and Freundlich isotherm. Kinetic studies were carried out, where the data were analyzed using pseudo first-order and pseudo second-order equations. Studies on thermodynamics were done where the thermodynamic parameters such as ΔH^0 , ΔS^0 , ΔG^0 ; activation parameters (ΔH^* , ΔS^* , ΔG^*) and activation energy (E_a) were determined.

1 Experimental

1.1 Chemicals

All reagents (Merck, Germany) used were of analytical grade and are as the following: $FeCl_2(H_2O)_4$ (99%), $FeCl_3$ (99%), Fe_2O_3 (99%), HCl (fuming, 37%), HNO_3 (65%), H_2O_2 (30%), ICP multi-element standard solution (1000 mg/L), $KMnO_4$ (99%), $MnCl_2(H_2O)_4$ (99.5%), and NaOH (99%). Solutions were prepared using de-ionized (DI) water from Millipore system with a resistivity of 18.9 M Ω .

1.2 Sample preparation

Silica sand with a grain size of 0.853 to 1.20 mm was soaked in 10% HNO_3 for 2 hr, rinsed with DI water, and dried at 105°C using a Channel Precision Oven model DV452 220V.

MOCS1 was prepared following a modified procedure of Eren et al. (2009). About 100 g of acid-washed sand was soaked in 2.0 mol/L NaOH solution for 2 hr at 90°C and filtered using a sieve. Then, the base-activated sand was stirred in 150 mL of 0.5 mol/L $MnCl_2$ where 300 mL of 0.5 mol/L NaOH was added drop wise. After which, 250 mL of 1.5 mol/L H_2O_2 was added and the suspension was

stirred at 30 r/min for 24 hr to promote coating. After 24 hr, the MnO_2 -coated sand was washed with DI water and dried at 90°C. The same procedure was done for MOCS2 but without the addition of H_2O_2 .

For the preparation of IOCS1, 25 g Fe_2O_3 and 100 g sand were stirred in 500 mL DI water at 30 r/min for 24 hr. The excess solution was decanted and the sand was washed with DI water. The Fe_2O_3 -coated sand was dried at 90°C.

For IOCS2, the procedure for coating sand with iron hydroxide is similar to the work of Ahammed and Meera (2010). Pre-washed sand (100 g) was mixed with 250 mL deionized water containing 50 g of $FeCl_3$. The slurry was dried at 90°C for 48 hr. After drying, 500 mL of 5 mol/L NaOH was added and the suspension was stirred at 30 r/min for 4 hr. The iron-coated sand was dried at 90°C for 24 hr. After drying, the coated sand was rinsed with DI water. The $Fe(OH)_3$ -coated sand was again dried at 90°C.

MIOCS was collected from Chunghua Water Treatment Plant located in central Taiwan. The MIOCS was obtained from the filter bed, where Fe and Mn oxides naturally coated the filter media over a long period of time. The adsorbent was sieved, rinsed with DI water and dried at 90°C.

1.3 Effect of pH

The uptake of Mn^{2+} under varying pH (5.5 to 8.0) and temperature (25°C to 45°C) was investigated. The adsorbent of (0.6250 \pm 0.0010) g with 25 mL of 10.0 mg/L Mn^{2+} solution was agitated at 120 r/min. After 24 hr, the residual Mn^{2+} concentration was determined using inductively coupled plasmaoptical emission spectrometry (ICP-OES, PerkinElmer DV2000 Series, USA).

1.4 Isotherm studies

A fixed amount of adsorbent was equilibrated under varying initial Mn^{2+} concentration (2.0 to 10.0 mg/L) using 120 r/min at pH 8 and 25°C. After 24 hr, the solution was analyzed in ICP-OES for the final concentration of Mn^{2+} .

Langmuir and Freundlich models were used in analyzing the isotherm data. Langmuir isotherm is based on the following assumptions: the model is valid only for monolayer adsorption, where all the binding sites have the same energy levels and can occupy one adsorbate molecule per site (Febrianto et al., 2009). The linear equation is given as Eq. (1):

$$\frac{1}{q_e} = \frac{1}{q_{mL}} + \frac{1}{bq_{mL}C_e} \quad (1)$$

where, q_{mL} (mg/g) is the maximum adsorption capacity at monolayer coverage and b (mL/mg) is the Langmuir equilibrium constant.

The Freundlich model is an empirical equation that describes a multi-site adsorption on energetically heterogeneous surfaces. The linearized form can be expressed as

Eq. (2):

$$\log q_e = \log K_F + \frac{1}{n} \log C_e \quad (2)$$

where, K_F and n are Freundlich constants, corresponding to relative adsorption capacity and adsorption intensity, respectively (Wan Ngah and Fatinathan, 2008).

1.5 Kinetics studies

The kinetics studies were conducted by adding a fixed amount of adsorbent into 25 mL of 10.0 mg/L Mn²⁺ solution under varying contact time (30 min to 24 hr) at 120 r/min and pH 8.0. In the kinetic study, the pseudo first- and second-order equations were used in evaluating the experimental data. The pseudo first-order (Lagergren) equation could be expressed as Eq. (3):

$$\log (q_e - q_t) = \log q_e - \frac{k_1}{2.303} t \quad (3)$$

where, k_1 (min⁻¹) is the rate constant, q_e (mg/g) and q_t (mg/g) are the adsorption capacity at equilibrium and at time, t (min), respectively (Benavente et al., 2011).

The linear form of the pseudo second-order equation is given as Eq. (4):

$$\frac{t}{q_t} = \frac{1}{k_2 q_e^2} + \frac{1}{q_e} t \quad (4)$$

where, k_2 (g/(mg·min)) is the pseudo second-order rate constant (Dinu and Dragan, 2010).

1.6 Thermodynamics studies

Adsorption thermodynamics was performed by varying the temperature (25 to 45°C) and contact time (30 min to 24 hr). In this experiment, (0.6250 ± 0.0010) g adsorbent and 25 mL of 10.0 mg/L Mn²⁺ solution were agitated at 120 r/min.

The thermodynamic parameters such as activation energy, ΔG^0 , ΔS^0 , ΔH^0 , ΔG^* , ΔS^* and ΔH^* were obtained. The activation energy refers to the minimum amount of energy that must be overcome in order for adsorption to proceed. The value of the activation energy can be determined experimentally using the rate constants at various temperatures according to the Arrhenius equation:

$$\ln k = \ln A - \frac{E_a}{RT} \quad (5)$$

where, k is the rate constant, A is a constant called the pre-exponential or frequency factor, E_a (kJ/mol) is the activation energy, R (8.314 J/(mol·K)) is the gas constant, and T (K) is the absolute temperature (Ferreiro and de Bussetti, 2007).

The thermodynamic parameters would describe whether the adsorption process follows an activated complex or not. The graphical procedure in obtaining the values of

these parameters is explained using the Eyring equation as follows:

$$\ln \left(\frac{k}{T} \right) = \ln \frac{k_B}{h} + \frac{\Delta S^*}{R} + \frac{\Delta H^*}{T} \quad (6)$$

where, k_B (1.3807×10^{-23} J/K) is the Boltzman constant, h (6.621×10^{-34} Js) is the Planck constant. The values of ΔH^* and ΔS^* can be obtained from the slope and intercept of the plot of $1/T$ vs. $\ln(k/T)$, and the value of ΔG^* is obtained from Eq. (7):

$$\Delta G^* = \Delta H^* - T\Delta S^* \quad (7)$$

In order to evaluate whether the adsorption process is spontaneous or not, the thermodynamic parameters of adsorption are needed. The Gibb's free energy ΔG of adsorption is used as an indication of spontaneity of the process and is given by the relation:

$$\Delta G^0 = \Delta H^0 - T\Delta S^0 \quad (8)$$

where, ΔG is given by the Van't Hoff equation:

$$\Delta G^0 = -RT \ln K_{ads} \quad (9)$$

where, K_{ads} is the equilibrium constant equal to the Langmuir equilibrium constant b .

2 Results and discussion

2.1 Effect of pH

Figure 1 illustrates the effect of pH on the adsorption capacity of greensand in the removal of Mn²⁺. In all five adsorbents, the removal of Mn²⁺ was observed to be lowest at pH 5.5. In general, the capacity of the adsorbents was observed to increase with an increase in pH from 5.5 to 8, where MIOCS and IOCS1 exhibited the highest and lowest capacities over the entire range, respectively. Thus, as the pH becomes more basic, an increase in adsorption capacity of the adsorbents was observed as well. This increase is observed in the order of MIOCS > MOCS1 > MOCS2 > IOCS2 > IOCS1.

It can be seen that the capacity of Mn-greensand (MOCS1 and MOCS2) was higher over a wider range of pH compared to that of Fe-greensand (IOCS1 and IOCS2). This is due to the reported PZC of manganese oxides (pH 1.4–5.5), which is higher than iron oxides (pH 6–10) (Qin et al., 2011). In the pH range of 5.5–8.0, the surface of Mn-greensand was negatively charged while the surface of Fe-greensand was positively-charged from pH 5.5 to 6.0. At pH > 6.0, the surface of Fe-greensand becomes negatively-charged. In comparison to Fe-greensand, the more negatively charged surface of Mn-greensand would have higher affinity towards Mn²⁺ that makes the adsorption more favourable, which resulted to a higher adsorption capacity.

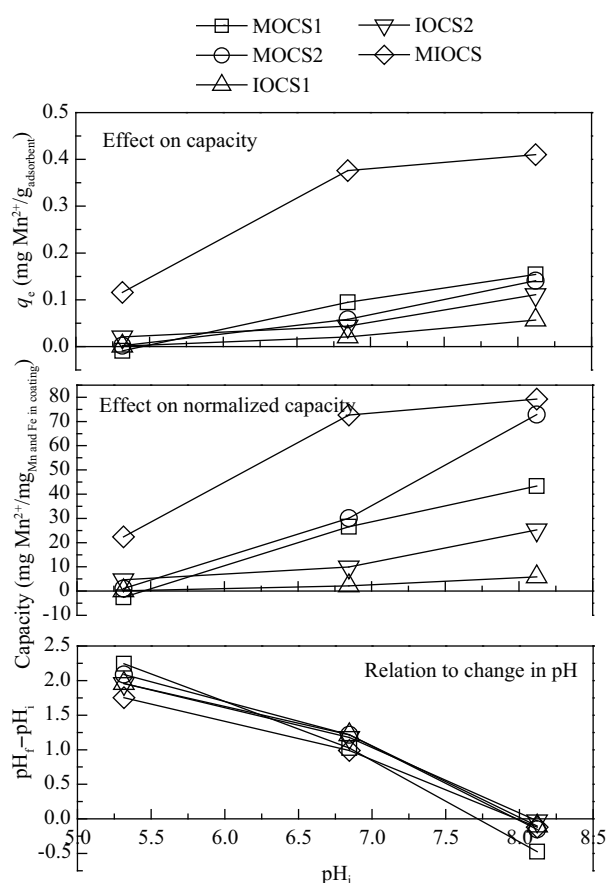


Fig. 1 Effect of initial pH on the adsorption capacity (a), normalized adsorption capacity of Mn²⁺ on greensand (b), and the relation to the change in pH of solution (c). Experimental conditions: initial Mn²⁺ 10 mg/L, adsorbent dosage 0.625 g, volume 25 mL, 24 hr, 25°C, 120 r/min. The y-axis for Fig. 1b refers to the mg of Mn²⁺ per mg of Mn and Fe coating. pH_f and pH_i refer to final and initial pH, respectively.

2.2 Effect of temperature

In Fig. 2, the effect of temperature on the adsorption capacity of the adsorbents is illustrated. Results showed that the equilibrium capacities of greensand increased with temperature, which indicates that the process is endothermic. The degree of increase from 25 to 35°C was higher compared to that from 35 to 45°C. The adsorption capacity of MIOCS was consistently high and stable. At 45°C, MOCS1, MOCS2, and IOCS2 performed similarly to MIOCS as their capacities were tripled from 25°C. A substantial improvement in the performance of IOCS1 was observed as it incurred the highest increase in capacity,

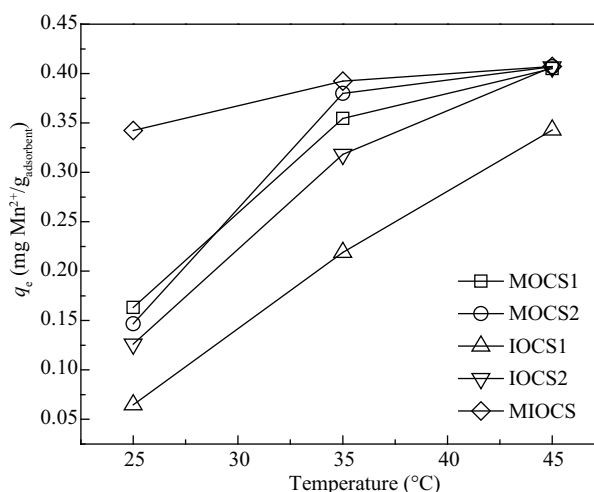


Fig. 2 Adsorption capacity of greensand for Mn²⁺ at different temperatures. Experimental conditions: initial Mn²⁺ 10 mg/L, adsorbent dosage 0.625 g, pH 8, volume 25 mL, 24 hr, 120 r/min.

although still consistently the lowest compared to the other adsorbents.

2.3 Isotherm studies

Isotherm studies were conducted to provide information on the capacity of the adsorbents under different concentrations of Mn²⁺. The equilibrium data were analyzed using the Langmuir and Freundlich model.

The calculated Langmuir and Freundlich parameters related to the adsorption of Mn²⁺ in greensand are presented in Table 1. Both isotherms were found to be linear over the entire concentration range as indicated by their high R^2 values (0.945 to 0.994) and the linearized isotherm plots shown in Fig. 3. The high correlation to both Langmuir and Freundlich isotherms implies a monolayer adsorption and the existence of heterogeneous surface in the adsorbents, respectively. However, higher R^2 values were reported with Langmuir isotherm for all adsorbents except MIOCS. This means that the Langmuir isotherm could provide a better model for the adsorption system compared to the Freundlich isotherm. The value of b (L/mg Mn²⁺) represents the adsorption constant and gave an idea of the affinity of Mn²⁺ to the binding sites. Results showed the highest affinity of Mn²⁺ to MIOCS, and surprisingly the least affinity to MOCS1. However the value of b is highly related to the extent of coverage of the available adsorption sites. Therefore, a high value of b could be observed even

Table 1 Langmuir and Freundlich parameters for the adsorption of Mn²⁺

Adsorbent	Langmuir			Freundlich		
	b (L/mg Mn ²⁺)	q_{mL} (mg Mn ²⁺ /g)	R^2	n	K_F ((mg Mn/g) (L/mg Mn ²⁺) ^{1/n})	R^2
MOCS1	0.027	2.617	0.989	1.05	0.0688	0.989
MOCS2	0.084	0.830	0.992	1.40	0.0746	0.973
IOCS1	0.076	0.408	0.966	1.19	0.0287	0.945
IOCS2	0.141	0.553	0.994	1.60	0.0806	0.980
MIOCS	1.656	0.884	0.959	2.75	0.4817	0.964

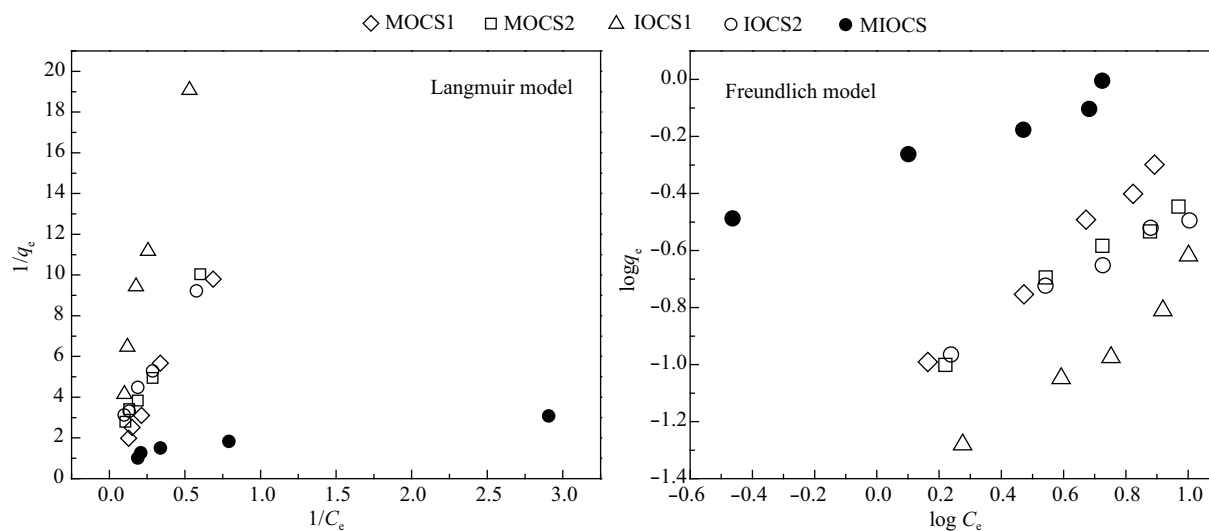


Fig. 3 Isotherms plots using Langmuir and Freundlich models for the adsorption of Mn^{2+} using greensand. Experimental conditions: initial Mn^{2+} 2–10 mg/L, adsorbent dosage 0.125 g, volume 25 mL, pH 8, 24 hr, 25°C, 120 r/min.

for adsorbents with a very low number of adsorption sites.

2.4 Kinetic studies

In order to determine the rate-limiting step, kinetic models such as pseudo first-order, and pseudo second-order equation were employed to evaluate the experimental data.

Figure 4 illustrates the actual kinetic data plots of the adsorbents under temperature range 25–45°C. The corresponding parameters and coefficient of determination of the curves are summarized in **Table 2** using the pseudo first- and second-order kinetic model. The corresponding values of R^2 are observed to be the highest for the pseudo second-order. Thus the pseudo second-order equation provided a better kinetic model for the adsorption of Mn^{2+}

using greensand at 25 to 45°C (with the exception of IOCS1 at 45°C). This implies that the adsorption might be governed by chemisorption which involved the formation of covalent bonds that enabled sharing or exchange of electrons between Mn^{2+} and the adsorbent molecules (Futalan et al., 2011; Taffarel and Rubio, 2010). A chemisorption mechanism only allows for a monolayer adsorption, which is in good agreement with Langmuir model that best describes the equilibrium adsorption data. Conversely, the correlation with the pseudo first-order kinetic model resulted in significantly low R^2 values at 25°C and 35°C, whereas an acceptable correlation with the pseudo first-order was observed when the temperature was increased to 45°C.

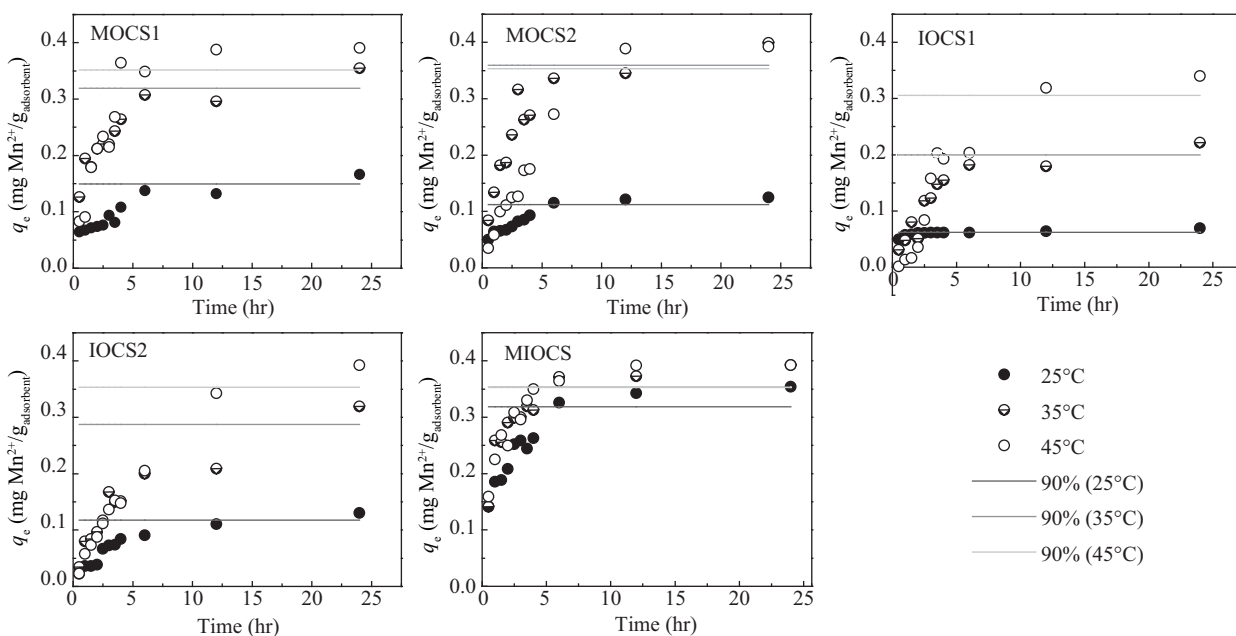


Fig. 4 Actual kinetic data plots for the adsorption of Mn^{2+} at 25, 35, and 45°C. Experimental conditions: initial Mn^{2+} 10 mg/L, volume 25 mL, pH 8, 24 hr, 120 r/min.

Table 2 Pseudo first- and second-order kinetic model parameters for the adsorption of Mn^{2+} at different temperatures

Temperature	Adsorbent	Pseudo first-order			Pseudo second-order		
		$q_{e, \text{theo}}$ (mg/g)	k_1 (min^{-1})	R^2	$q_{e, \text{theo}}$ (mg/g)	k_2 (g/(mg·min))	R^2
25°C	MOCS1	0.106	0.115	0.7241	0.178	2.220	0.9777
	MOCS2	0.092	0.288	0.9523	0.133	4.907	0.9959
	IOCS1	0.012	0.085	0.6157	0.069	36.222	0.9986
	IOCS2	0.797	0.149	0.9309	0.150	1.782	0.9845
	MIOCS	0.228	0.266	0.9485	0.374	2.052	0.9977
35°C	MOCS1	0.181	0.122	0.6976	0.367	1.775	0.9926
	MOCS2	0.245	0.153	0.7260	0.429	1.119	0.9951
	IOCS1	0.152	0.135	0.6811	0.257	1.001	0.9432
	IOCS2	0.245	0.081	0.7670	0.362	0.552	0.9548
	MIOCS	0.171	0.212	0.8048	0.406	2.792	0.9992
45°C	MOCS1	0.413	0.418	0.9167	0.437	1.026	0.9853
	MOCS2	0.739	0.399	0.9358	0.543	0.240	0.9559
	IOCS1	0.437	0.245	0.9582	-0.301	0.114	0.0400
	IOCS2	0.437	0.172	0.9745	0.567	0.177	0.9783
	MIOCS	0.367	0.540	0.9713	0.409	2.841	0.999

2.5 Thermodynamics studies

In the previous section, the adsorption with MIOCS was determined to be endothermic and that with the rest of the adsorbents was exothermic. This would be validated in this part of the study by calculating the values of thermodynamic parameters namely the activation energy (E_a), the activation parameters (ΔH^* , ΔG^* , ΔS^*), and the thermodynamic parameters (ΔH^0 , ΔG^0 , ΔS^0) of the adsorption process.

The activation energies E_a were calculated from the slope of the Arrhenius plots, as shown in **Fig. 5**. The values of the activation energy and the coefficients of determination of the curves are summarized in **Table 3**. In all adsorbents, the linear correlation gave reasonably high R^2 values. The negative value of the activation energy means that the adsorption proceeded without energy barrier, where it could proceed spontaneously. However, the negative activation energy also means that temperature did not favor the adsorption process to proceed on a faster rate. This validates the adsorption behaviour of MOCS1, MOCS2, and IOCS2, where their rate constants decreased as the temperature increased from 25°C to 45°C. This indicates that the Mn^{2+} ions can move and attach freely to the adsorption sites, but the increase in temperature also increased the velocity of the ions such that the probability of successful attachment to the adsorption sites was decreased. This is a characteristic of an exothermic adsorption process, wherein the Mn^{2+} ions become more soluble at higher temperature. This results to Mn^{2+} ions experiencing stronger interaction forces with the solvent than with the adsorbent, which makes it more difficult for adsorption to occur. On the contrary, with MIOCS, the positive value of its activation energy signified the presence of an energy barrier. An increase in temperature therefore provided the energy for the ions to overcome this energy barrier, resulting in faster adsorption.

Consistent with the findings in the kinetics studies when

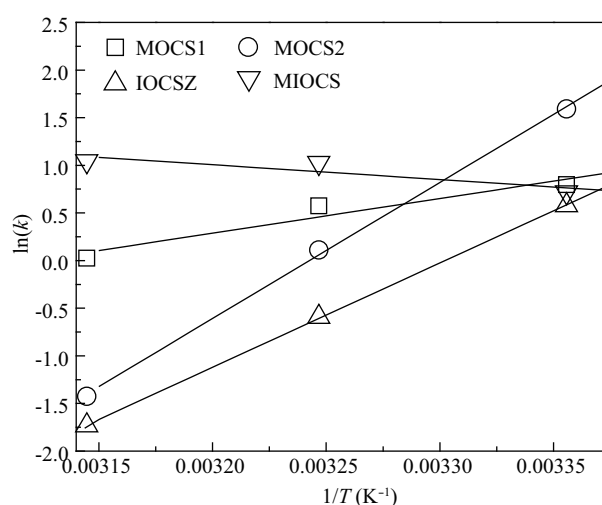


Fig. 5 Arrhenius plots for the adsorption of Mn^{2+} using greensand. Experimental conditions: initial Mn^{2+} 10 mg/L, adsorbent dosage 0.625 g, pH 8, 24 hr, 120 r/min.

the adsorption was established to be pseudo second-order, the magnitudes of the E_a suggested that the mechanism of adsorption was chemisorption since they are higher than

Table 3 Activation energies (E_a) for the adsorption of Mn^{2+} using greensand

Adsorbent	Temperature (K)	k_2 (g/(mg·min))	R^2	E_a (kJ/mol)
MOCS1	298	2.22	0.935	-30.25
	308	1.78		
	318	1.03		
MOCS2	298	4.91	0.999	-118.77
	308	1.12		
	318	0.24		
IOCS2	298	1.78	0.999	-91.01
	308	0.55		
	318	0.18		
MIOCS	298	2.05	0.806	12.95
	308	2.79		
	318	2.84		

the activation energy for physisorption, which does not usually exceed 4.2 kJ/mol.

The activation parameters ΔH^* , ΔG^* , and ΔS^* were calculated using the Eyring equation, where values are listed in **Table 4**. This will determine if the adsorption process followed an activated complex prior to final sorption.

High values of correlation to the Eyring equation were obtained, except for MIOCS which only resulted in an R^2 value of 0.726. However, this value of R^2 can be acceptable especially since the Eyring equation is not strictly linear with respect to $1/T$.

In general, the free energy of activation ΔG^* were positive in all temperatures, which indicates that the activation was accompanied by an external energy source for the adsorption to proceed. This may refer to the energy needed for the Mn^{2+} ions to overcome the activation energy or to form an activated complex while the ions were in the transition state.

In all the adsorbents, results showed a negative value of the entropy of activation ΔS^* . The negative value of ΔS^* suggested the manifestation of an associative chemisorption through the formation of an activated complex between the Mn^{2+} ions and adsorbents. The formation of these covalent bonds was exothermic and involved the release of energy resulting in a decrease in enthalpy. Thus, the enthalpy of activation ΔH^* for MOCS1, MOCS2, and

IOCS2 was negative and higher in magnitude than their corresponding activation energies. For MIOCS, the value of its ΔH^* was also positive but lower in magnitude than its activation energy. This means that while in transition state, Mn^{2+} ions released heat by forming an activated complex with the adsorbent. In general, the adsorption of Mn^{2+} onto greensand involved the formation of an activated complex. This is consistent with the previous findings that the adsorption was governed by a chemisorption mechanism.

The thermodynamic parameters, ΔH^0 , ΔG^0 , and ΔS^0 of the system were determined using the Van't Hoff equation to evaluate the spontaneity of the adsorption process. In **Table 5**, the results showed that adsorption process using MOCS1, MOCS2, and IOCS2 was exothermic as indicated by the negative sign of the ΔH^0 values, whereas the adsorption process using MIOCS was endothermic as indicated by the positive value of its ΔH^0 . This is consistent with their E_a values. For the endothermic characteristic of adsorption with MIOCS, it means that the magnitude of the total energy absorbed by the system due to bond breaking was greater to the magnitude of the total energy released due to bond making. The reverse is true for the exothermic adsorption with MOCS1, MOCS2, and IOCS2. The bond breaking energy might be associated with the displacement of previously adsorbed molecules from the surface of the adsorbents, such as water or other functional

Table 4 Activation parameters for the adsorption of Mn^{2+} onto greensand

Adsorbent	Temperature (K)	k (g/(mol·sec))	R^2	ΔH^* (kJ/mol)	ΔS^* (kJ/(mol·K))	ΔG^* (kJ/mol)
MOCS1	298	2.033	0.944	-32.81	-0.35	71.1
	308	1.626				74.6
	318	0.940				78.1
MOCS2	298	4.493	0.999	-121.33	-0.64	69.2
	308	1.024				75.6
	318	0.220				82.0
IOCS	298	1.632	0.999	-93.57	-0.55	71.8
	308	0.506				77.3
	318	0.162				82.8
MIOCS	298	1.878	0.726	10.39	-0.20	71.3
	308	2.556				73.4
	318	2.602				75.4

Table 5 Thermodynamic parameters for the adsorption of Mn^{2+} using greensand

Adsorbent	Temperature (K)	K_{ads}	ΔG^0 (kJ/mol)	ΔH^0 (kJ/mol)	ΔS^0 (kJ/(mol·K))	R^2
MOCS1	298	2.220	-1.98	-30.55	-0.095	0.932
	308	1.775	-1.47			
	318	1.026	-0.07			
MOCS2	298	4.910	-3.94	-118.97	-0.386	0.999
	308	1.120	-0.29			
	318	0.240	3.77			
IOCS2	298	1.780	-1.43	-90.27	-0.298	1.000
	308	0.550	1.53			
	318	0.180	4.53			
MIOCS	298	2.050	-1.78	12.72	0.049	0.849
	308	2.790	-2.63			
	318	2.840	-2.76			

groups like H^+ or OH^- . The bond making energy might be associated with the formation of activated complex and the final sorption of Mn^{2+} ions onto the surface of the adsorbents.

According to Ferreiro and de Bussetti (2007), physisorption involves enthalpy changes in the range of 2.1–20.9 kJ/mol while chemisorption involved enthalpy changes in the range of 100–500 kJ/mol. Based on the values of ΔH , the adsorption using MOCS2 and IOCS2 followed a chemisorption mechanism. On the other hand, the values suggest that the adsorption using MOCS1 probably involved a physical-chemical mechanism and that with MIOCS was purely physical. The case for MOCS1 and MIOCS was contrary to their E_a values suggesting the chemical nature of adsorption with these adsorbents. Thus it can be said that the adsorption involving MOCS1 and MIOCS involved a physical-chemical mechanism and not purely physical or chemical. The negative value of ΔS suggested the decrease in randomness in the system as the Mn^{2+} ions got adsorbed onto the adsorbents.

The negative value of ΔG means the adsorption process was spontaneous. MOCS1 and MIOCS exhibited a spontaneous adsorption of Mn^{2+} in all temperatures from 25–35°C, MOCS2 at 25 and 35°C, and IOCS2 exhibited spontaneity of adsorption of Mn^{2+} only at 25°C. Adsorption with MOCS1, MOCS2, and IOCS2 was more spontaneous at lower temperatures as their ΔG^0 value became more negative when the temperature was lowered from 45 to 25°C. This is supported by the fact that these adsorbents exhibited an exothermic adsorption. The ΔG^0 of MIOCS became more negative when the temperature was increased from 25 to 45°C, meaning the adsorption was more favorable at higher temperatures since the adsorption using this adsorbent was endothermic.

3 Conclusions

In this study, the adsorption of Mn^{2+} using various iron oxide and manganese oxide-coated sand namely MOCS1, MOCS2, IOCS1, IOCS2, and MIOCS was investigated. Manganese and iron oxides can be successfully coated onto sand using the impregnation methods performed. Solution pH has a significant influence in the adsorption of Mn^{2+} , where the capacity of the adsorbents increases with increasing pH from 5.5 to 8.0. In general, manganese oxides have higher adsorption capability for Mn^{2+} than iron oxides.

Temperature is also a significant factor, where the Mn^{2+} uptake increases with increasing temperature from 25 to 45°C. In all adsorbents, the adsorption equilibrium with all adsorbents follows both the Langmuir and Freundlich isotherms while kinetic studies show to follow the pseudo second-order equation. The adsorption with MIOCS is exothermic because the kinetic rate decreases with increasing temperature. The adsorption with the other

adsorbents is exothermic because the kinetic rates decrease with increasing temperature. The values of the activation energy and enthalpy change confirmed that adsorption with MIOCS is endothermic, and that the adsorption with the rest of the adsorbents (except IOCS1) are exothermic. The values of the activation energy and enthalpy change suggested that adsorption with MIOCS and MOCS1 is governed by physisorption and chemisorption mechanisms and that of MOCS2 and IOCS2 involves purely chemisorption mechanism. Adsorption of Mn^{2+} using MOCS and MIOCS is spontaneous from 25 to 45°C. With MOCS2, the adsorption is spontaneous at 25 to 35°C. With IOCS2, the adsorption is spontaneous only at 25°C. Since adsorption with MOCS1, MOCS2, and IOCS2 are exothermic, it follows that the adsorption using these adsorbents are more spontaneous at lower temperatures. Since adsorption with MIOCS is endothermic, the adsorption using this adsorbent is more spontaneous at higher temperatures. Conclusively, all the adsorbents (except IOCS1) are viable for use in removing dilute Mn^{2+} from aqueous solution.

Acknowledgments

The authors would like to acknowledge the Philippine ERDT scholarship and Taiwan National Science Council (NSC 101-2221-E-041-007) for their financial support.

References

- Ahmed M M, Meera V, 2010. Metal oxide/hydroxide-coated dualmedia filter for simultaneous removal of bacteria and heavy metals from natural waters. *Journal of Hazardous Materials*, 181(1-3): 788–793.
- Benavente M, Moreno L, Martinez J, 2011. Sorption of heavy metals from gold mining wastewater using chitosan. *Journal of the Taiwan Institute of Chemical Engineers*, 42(6): 976–988.
- Benjamin M M, Sletten R S, Bailey R P, Bennett T, 1996. Sorption and filtration of metals using iron-oxide-coated sand. *Water Research*, 30(11): 2609–2620.
- Buamah R, Petrusevski B, Schippers J C, 2008. Adsorptive removal of manganese(II) from the aqueous phase using iron oxide coated sand. *Journal of Water Supply: Research and Technology-AQUA*, 57(1): 1–11.
- Chang Y Y, Song K H, Yang J K, 2008. Removal of As(III) in a column reactor packed with iron-coated sand and manganese-coated sand. *Journal of Hazardous Materials*, 150(3): 565–572.
- Dinu M V, Dragan E S, 2010. Evaluation of Cu^{2+} , Co^{2+} and Ni^{2+} ions removal from aqueous solution using a novel chitosan/clinoptilolite composite: Kinetics and isotherm. *Chemical Engineering Journal*, 160(1): 157–163.
- Ellis D, Bouchard C, Lantagne G, 2000. Removal of iron and manganese from groundwater by oxidation and microfiltration. *Desalination*, 130(3): 255–264.
- Eren E, Afsin B, Onal Y, 2009. Removal of lead ions by acid activated and manganese oxide-coated bentonite. *Journal of Hazardous Materials*, 161(2-3): 677–685.
- Febrianto J, Kosasih A N, Sunarso J, Ju Y H, Indraswati N, Is-

- madji S, 2009. Equilibrium and kinetic studies in adsorption of heavy metals using biosorbent: A summary of recent studies. *Journal of Hazardous Materials*, 162(2-3): 616–645.
- Ferreiro E A, de Bussetti S G, 2007. Thermodynamic parameters of adsorption of 1,10-phenantroline and 2,2'-bipyridyl on hematite, kaolinite and montmorillonites. *Colloids and Surfaces A: Physicochemical and Engineering Aspects*, 301(1-3): 117–128.
- Futalan C M, Kan C C, Dalida M L, Hsieh K J, Pascua C, Wan M W, 2011. Comparative and competitive adsorption of copper, lead, and nickel using chitosan immobilized on bentonite. *Carbohydrates Polymer*, 83(2): 528–536.
- Han R P, Zou W H, Zhang Z P, Shi J, Yang J J, 2006. Removal of copper(II) and lead(II) from aqueous solution by manganese oxide coated sand: I. Characterization and kinetic study. *Journal of Hazardous Materials*, 137(1): 384–395.
- Hu P Y, Hsieh Y H, Chen J C, Chang C Y, 2004. Characteristics of manganese-coated sand using SEM and EDAX analysis. *Journal of Colloid and Interface Science*, 272(2): 308–313.
- Kim W G, Kim S J, Lee S M, Tiwari D, 2009. Removal characteristics of manganese-coated solid samples for Mn(II). *Desalination and Water Treatment*, 4(1-3): 218–223.
- Lai C H, Lo S L, Chiang H L, 2000. Adsorption/desorption properties of copper ions on the surface of iron-coated sand using BET and EDAX analyses. *Chemosphere*, 41(8): 1249–1255.
- Lee C I, Yang W F, Hsieh C I, 2004. Removal of copper(II) by manganese-coated sand in a liquid fluidized-bed reactor. *Journal of Hazardous Materials*, 114(1-3): 45–51.
- Li E, Zeng X Y, Fan Y H, 2009. Removal of chromium ion(III) from aqueous solution by manganese oxide and microemulsion modified diatomite. *Desalination*, 238(1-3): 158–165.
- Phatai P, Wittayakun J, Grisanurak N, Chen W H, Wan M W, Kan C C, 2010. Removal of manganese ions from synthetic groundwater by oxidation using $KMnO_4$ and characterization of produced MnO_2 particles. *Water Science and Technology*, 62(8): 1719–1726.
- Piispänen J K, Sallanko J T, 2010. Mn(II) removal from groundwater with manganese oxide-coated filter media. *Journal of Environmental Science and Health, Part A: Environmental Science*, 45(13): 1732–1740.
- Qin Q D, Wang Q Q, Fu D F, Ma J, 2011. An efficient approach for Pb(II) and Cd(II) removal using manganese dioxide formed *in situ*. *Chemical Engineering Journal*, 172(1): 68–74.
- Taffarel S R, Rubio J, 2010. Removal of Mn^{2+} from aqueous solution by manganese oxide coated zeolite. *Minerals Engineering*, 23(14): 1131–1138.
- Teng Z, Huang J Y, Fujita K, Takizawa S, 2001. Manganese removal by hollow fiber micro-filter. Membrane separation for drinking water. *Desalination*, 139(1-3): 411–418.
- Tiwari D, Laldanwngliana C, Choi C H, Lee S M, 2011. Manganese-modified natural sand in the remediation of aquatic environment contaminated with heavy metal toxic ions. *Chemical Engineering Journal*, 171(3): 958–966.
- Wan Ngah W S, Fatinathan S, 2008. Adsorption of Cu(II) ions in aqueous solution using chitosan beads, chitosan-GLA beads and chitosan-alginate beads. *Chemical Engineering Journal*, 143(1-3): 62–72.

JOURNAL OF ENVIRONMENTAL SCIENCES

环境科学学报(英文版)
(<http://www.jesc.ac.cn>)

Aims and scope

Journal of Environmental Sciences is an international academic journal supervised by Research Center for Eco-Environmental Sciences, Chinese Academy of Sciences. The journal publishes original, peer-reviewed innovative research and valuable findings in environmental sciences. The types of articles published are research article, critical review, rapid communications, and special issues.

The scope of the journal embraces the treatment processes for natural groundwater, municipal, agricultural and industrial water and wastewaters; physical and chemical methods for limitation of pollutants emission into the atmospheric environment; chemical and biological and phytoremediation of contaminated soil; fate and transport of pollutants in environments; toxicological effects of terrorist chemical release on the natural environment and human health; development of environmental catalysts and materials.

For subscription to electronic edition

Elsevier is responsible for subscription of the journal. Please subscribe to the journal via <http://www.elsevier.com/locate/jes>.

For subscription to print edition

China: Please contact the customer service, Science Press, 16 Donghuangchenggen North Street, Beijing 100717, China. Tel: +86-10-64017032; E-mail: journal@mail.sciencep.com, or the local post office throughout China (domestic postcode: 2-580).

Outside China: Please order the journal from the Elsevier Customer Service Department at the Regional Sales Office nearest you.

Submission declaration

Submission of an article implies that the work described has not been published previously (except in the form of an abstract or as part of a published lecture or academic thesis), that it is not under consideration for publication elsewhere. The submission should be approved by all authors and tacitly or explicitly by the responsible authorities where the work was carried out. If the manuscript accepted, it will not be published elsewhere in the same form, in English or in any other language, including electronically without the written consent of the copyright-holder.

Submission declaration

Submission of the work described has not been published previously (except in the form of an abstract or as part of a published lecture or academic thesis), that it is not under consideration for publication elsewhere. The publication should be approved by all authors and tacitly or explicitly by the responsible authorities where the work was carried out. If the manuscript accepted, it will not be published elsewhere in the same form, in English or in any other language, including electronically without the written consent of the copyright-holder.

Editorial

Authors should submit manuscript online at <http://www.jesc.ac.cn>. In case of queries, please contact editorial office, Tel: +86-10-62920553, E-mail: jesc@263.net, jesc@rcees.ac.cn. Instruction to authors is available at <http://www.jesc.ac.cn>.

Journal of Environmental Sciences (Established in 1989)

Vol. 25 No. 7 2013

Supervised by	Chinese Academy of Sciences	Published by	Science Press, Beijing, China
Sponsored by	Research Center for Eco-Environmental Sciences, Chinese Academy of Sciences	Distributed by	Elsevier Limited, The Netherlands
Edited by	Editorial Office of Journal of Environmental Sciences P. O. Box 2871, Beijing 100085, China Tel: 86-10-62920553; http://www.jesc.ac.cn E-mail: jesc@263.net , jesc@rcees.ac.cn	Domestic	Science Press, 16 Donghuangchenggen North Street, Beijing 100717, China Local Post Offices through China
Editor-in-chief	Hongxiao Tang	Foreign	Elsevier Limited http://www.elsevier.com/locate/jes
CN 11-2629/X	Domestic postcode: 2-580	Printed by	Beijing Beilin Printing House, 100083, China
		Domestic price per issue	RMB ¥ 110.00

ISSN 1001-0742



9 771001 074130